AN INVESTIGATION OF THE NEUTRON DETECTION EFFICIENCY
OF A PLASTIC SCINTILLATION DETECTOR IN THE ENERGY RANGE 6 TO 41 MeV*

M. W. McNAUGHTON, F. P. BRADY, W. B. BROSTE, A. L. SAGLE† and S. W. JOHNSEN†

*Crocker Nuclear Laboratory and Physics Department, University of California,
Davis, California 95616, U.S.A.*

Measurements of ±3% accuracy are reported of the detection efficiency of a 15.2 cm thick NE102A plastic scintillation detector in the energy range 6 to 41 MeV, for thresholds of 1.0 and 4.2 MeV. The results are compared with the predictions of two computer codes, and significant discrepancies of up to 20% are observed. The variation of efficiency across the face of the detector has been measured and differences of about 10% (relative) observed between centre and edge of 7.1 cm diameter cylinder.

1. Introduction

Experiments in nuclear physics that attempt to measure cross sections by detecting one or more neutrons are often limited in the accuracy they can attain by an inadequate knowledge of the neutron detection efficiency of the detector. In the case of differential cross section measurements a knowledge of the variation of efficiency with the energy of the neutron incident on the detector is required. The present experiment was necessitated by an attempt to measure the differential cross section for elastic scattering of neutrons by protons at 25 and 50 MeV to an accuracy of ±4% or better. In that experiment[1] the error in forward angle data was dominated by the uncertainty of detector efficiency, an uncertainty which the present experiment greatly reduced.

2. Definition of the detection efficiency

The efficiency, ε, of a neutron detector to neutrons of a given energy is the probability of such a neutron, incident on the detector within some effective area S, producing an acceptable pulse in the attendant electronics, sufficient to enable its presence to be detected (and distinguished from noise). In case of detection in a plastic scintillator (such as in the present experiment), the neutron must transfer sufficient energy to a charged particle so that the scintillation light collected by the photomultiplier produces a pulse above the electronic detection threshold. The efficiency of the detector therefore depends on the type, shape and size of the scintillator, the energy of the neutron, and the electronic detection threshold.

It cannot be assumed that the detection efficiency is constant across the face of the scintillator, nor that the true effective area (from which the solid angle is derived) is necessarily the area of the scintillator. Neutrons incident close to the edge of the scintillator may scatter across the boundary (either into or out of the scintillator) while charged particles receiving momentum close to the edge may similarly enter or leave, depositing only part of their kinetic energy within the scintillator. Furthermore, light collection may not be uniform across the detector face. The actual quantity required in the extraction of cross section data is the integrated product of efficiency ε and the surface area s: $\int \varepsilon(s) \, ds$.

3. Experimental method

Neutrons incident on the face of the detector may be "tagged" by generating the neutrons in a scattering or reaction process and flagging the presence of a neutron by detecting an associated charged particle in coincidence at the conjugate angle. The problem is complicated by the fact that the intensity distribution, I, of the flagged neutrons will not be uniform over the detector face. The crude measured efficiency, ε_1, equal to the quotient (detected neutrons) / (detected + flagged neutrons) may be expressed for a cylindrically symmetric detector

$$\varepsilon_1 = \frac{1}{I_t} \int I(r) \, \varepsilon(r) \, ds, \qquad (1)$$

where I and ε are written as functions of r, the radial distance from the cylinder axis, $(ds = 2\pi r \, dr)$, and the total neutron intensity

$$I_t = \int I(r) \, ds.$$

25

$I(r)$ may be calculated from a knowledge of the geometry of the apparatus using a Monte Carlo type program. Then, by measuring the relative efficiency profile of the detector, $\varepsilon_r(r)$, in addition to ε_1, the value of ε_1 may be used to determine the normalisation factor N in the relation

$$\varepsilon(r) = N\,\varepsilon_r(r). \qquad (2)$$

For most purposes it is convenient to define the "effective area" of the detector, S, to be equal to that of the scintillator, and calculate an effective mean efficiency, $\bar{\varepsilon}$, for this area, defined by

$$\bar{\varepsilon}S = \int \varepsilon(r)\,\mathrm{d}s.$$

Using eq. (1) and (2) we have

$$\bar{\varepsilon} = \frac{\varepsilon_1 S^{-1} \int \varepsilon_r(r)\,\mathrm{d}s}{I_t^{-1} \int \varepsilon_r(r)\,I(r)\,\mathrm{d}s}, \qquad (3)$$

$$(\mathrm{d}s = 2\pi r\,\mathrm{d}r).$$

4. The neutron detector

The neutron detector investigated in this experiment was one of several of identical specification. Each consisted of a right cylinder of NE102A, 7.1 cm diameter, 15.2 cm deep, mounted with its axis parallel to incident neutrons on an RCA 8575 phototube. Light collection was assisted by wrapping in aluminium foil, before light sealing with several layers of plastic tape. The absense of any substantial material surrounding the scintillator made the approximation of considering the effective area equal to the area of the scintillator a satisfactory one. Charged particles incident on the neutron detector were vetoed by a thin detector of NE102A plastic scintillator, in anticoincidence with the neutron detector.

5. Measurement of relative efficiency profile

The first part of the experiment consisted of an investigation of the relative detection efficiency $\varepsilon_r(r)$ across the (plane) face of the neutron detector. The detector was placed directly in the low flux ($< 4 \times 10^3$ n/s) neutron beams of various energies, formed by directing protons, H^+, or molecular hydrogen ions, H_2^+, onto targets of various thicknesses of ^7Li [2]), and collimating the resultant neutrons by means of a 5 mm square, 1 m long, steel collimator, into a beam 7 mm wide (fwhm) at the detector face. The spectrum of neutrons thus produced consisted of a high energy peak, 1.5 to 2 MeV wide, with a low-energy tail of low intensity.

A second neutron detector was fixed perpendicular to and in front of the first to act both as a monitor of the neutron beam intensity and an attenuator of the low-energy tail of the neutron beam. Incident neutron time-of-flight spectra were recorded for both detectors, and the peaks integrated to give the number of neutrons of the peak energy detected. To investigate its effectiveness, the monitor detector was tested for reproducibility and compared with the integrated readings of the Faraday cup into which protons emerging from the ^7Li target were swept by a clearing magnet.

Fig. 1 shows a typical set of data obtained by moving the detector relative to the beam, scanning the beam radially across the detector face, and determining the relative efficiency $\varepsilon_r(r)$ as the ratio of integrated peak counts in the moveable detector to that in the fixed monitor detector. By recording two-parameter spectra of incident time-of-flight vs neutron detector pulse height (NPH) and calibrating NPH with reference to the Compton edge of monoenergetic γ rays, the relative efficiency could be obtained simultaneously for several detector thresholds. Fig. 1 shows $\varepsilon_r(r)$ for thresholds of 1.0 MeV (^{60}Co), 2.0 MeV (linearly interpolated) and 4.2 MeV ($^{12}C^*$), in comparison with an empirical function, $\varepsilon_r = N(100 - 1.1r^2)$, ($r$ in cm).

The empirical function

$$\varepsilon_r = N(100 - ar^2), \qquad (4)$$

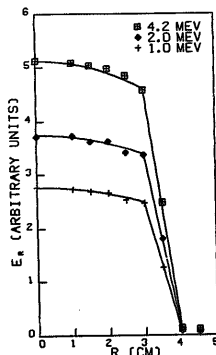(N normalisation, r in cm) produced a satisfactory fit

Fig. 1. Relative efficiency ε_r against radius r for thresholds of 1.0, 2.0 and 4.2 MeV. For $r \le 3$ cm, the curves are the empirical function [eq. (4)] with $a = 1.1$.

TABLE 1

Measured values of the coefficient a in eq. (4) (text) tabulated by neutron energy and detector threshold.

Neutron energy (MeV)	Detector threshold		
	1.0 MeV	2.0 MeV	4.2 MeV
10.0	1.1±0.1	1.3±0.1	4.0±0.4
12.8	1.1±0.1	1.1±0.1	2.0±0.2
20.0	1.1±0.1	1.1±0.1	1.1±0.1
30.0	1.1±0.1	1.1±0.1	1.1±0.1

TABLE 2

Mean detector efficiency $\bar{\varepsilon}$ [see text, eq. (3)] as a function of neutron energy and detection threshold.

Neutron energy (MeV)	Detector efficiency $\bar{\varepsilon}$ %	
	1.0 MeV threshold	4.2 MeV threshold
6.2	33.0±1.3	0.1±0.1
9.5	34.8±0.7	3.9±0.2
11.8	33.5±0.9	11.1±0.5
13.4	30.9±0.6	13.9±0.4
17.7	27.5±0.6	18.0±0.5
22.3	31.6±0.6	17.0±0.5
27.1	31.9±0.7	16.2±0.5
31.9	30.9±0.8	17.1±0.6
36.5	29.5±0.8	18.4±0.6
40.9	29.5±1.2	20.0±1.0

(generally better than 1%) to all profiles measured. Table 1 gives values of the coefficient a for the various energies and thresholds investigated.

6. Measurement of crude absolute efficiency ε_1

55 MeV neutrons produced by the same techniques as above[2]) were collimated by a 1.1 cm square steel collimator onto targets of $(CH_2)_n$ varying from 55 mg/cm^2 to 132 mg/cm^2 thick. Recoil protons were detected (and discriminated from heavier particles) by a telescope consisting of a 400 μm Si ΔE detector and a NaI E detector in coincidence. The E, ΔE and incident time-of-flight (INCTOF) signals were digitised, fed to a PDP15/40 computer via a CAMAC interface, and recorded, event by event, on magnetic tape.

Selecting protons by reference to the E vs ΔE correlation, and selecting the high-energy peak by reference to INCTOF, during analysis a peak of elastically scattered proton events (about 3 MeV broad) was seen standing on a background of <10% of events from C(n,p). A subtraction of events originating in carbon was made by recording data from a target of pure carbon (of nearly equivalent thickness, with a small correction for the different number of C nuclei), normalising the incident neutron flux via a triple detector neutron beam monitor telescope.

As a check of the ability of this system to selectively detect elastically scattered protons, the relative n–p differential cross section was extracted from this data. The results were in good agreement with 50 MeV data taken at this laboratory[1]).

With the ability to detect recoil protons from n–p elastic scattering, these events were used to flag the scattered neutron at the kinematically conjugate angle. The neutron detector was placed at the (relativistically) conjugate angle, with events being recorded for proton events both with and without a coincident neutron, and two further parameters, neutron detector pulse height

(NPH) and the relative time of the neutron to proton signal, fed through CAMAC to the computer and magnetic tape. As before the NPH parameter allowed different detector thresholds to be used during analysis, while the relative time parameter confirmed that accidental coincidences (with random time relationship) were negligible (<0.5%).

The crude efficiency ε_1 was calculated as the ratio of neutron events above the selected detection threshold in coincidence with protons from elastic n–p scattering, and the total of all elastically scattered protons detected. Measurements were made for a range of neutron energies, E_n, by altering the angles of the detectors relative to the beam, each measurement encompassing an energy spread of about ±1.5 MeV either side of the nominal neutron energy.

In order to improve statistical accuracy and to avoid the regions in which $\varepsilon_r(r)$ changes rapidly, the detector geometry was arranged so that for all n–p elastic events detected in the proton telescope, the conjugate neutron would enter and (if undeflected) leave the neutron detector through the front and rear walls, traveling the full depth of the detector.

7. The mean (effective) efficiency $\bar{\varepsilon}$

The conjugate flux distribution, $I(r)$, was calculated using a Monte-Carlo program. Successive events were simulated assuming uniform distribution of events over the proton beam spot in the ^{7}Li target, over the collimator area and over the face of the ΔE detector. The conjugate neutron direction was calculated for each event, and the radial distance r of the scattered neutron's interaction (within the detector) calculated, assuming an equal probability of interaction at any

depth within the detector. By this method the integrals of eq. (3) were determined to an accuracy better than 0.5%, and the mean efficiency $\bar{\varepsilon}$ over the area of the scintillator determined, ($\bar{\varepsilon}/\varepsilon_i$ being in the region of 0.95 except close to the detection threshold). Results are tabulated in table 2 and shown in relation to predictions of the version of Kurz's[3] code modified by Thornton and Smith[4]), and of Stanton's code[5]), in fig. 2.

8. Comparison with predicted efficiencies and discussion

The results displayed in fig. 2 indicate that the errors quoted by the authors[3, 5] for their predicted efficiencies, ±5% (Stanton) and ±10% (Kurz) are exceeded at certain neutron energies.

Previous comparisons between measured efficiencies and the predictions of Kurz's code have been reported [Thornton and Smith[4]), Wiegand et al.[6]), Young et al.[7]), Crabb et al.[8]), Hunt et al.[9]), and Parsons et al.[10])]. In general the same main features of disagreement are observed in these previous results and in fig. 2 of this present paper. Both measured and predicted efficiencies rise rapidly at threshold to a low-energy peak (dominated by neutron interactions with hydrogen in the scintillator); with increasing energy the efficiency falls as the n–p cross section falls, and then rises again as interactions with carbon begin to contribute; finally at higher energies the efficiency falls steadily as all contributing cross sections fall. The discrepancy between measurement and prediction consists predominantly of two features:

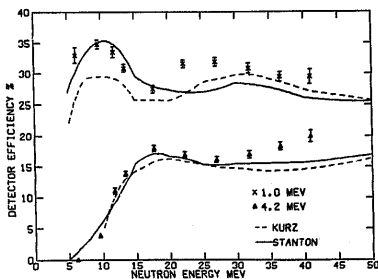1) the low-energy peak as predicted by Kurz rises to a lower maximum efficiency, especially at low thresh-

olds [cf. Thorton and Smith[4]), Hunt et al.[9])] (other measurements do not extend to this low energy);

2) the rise to the higher-energy peak begins at higher energy in the predicted curve of Kurz [cf. Wiegand et al.[6]), Young et al.[7]), Crabb et al.[8]) and Parsons et al.[10]) though the results of Hunt et al.[9]) do not show this].

The predictions of Stanton's code[5]) show improved agreement with experiment (fig. 2 and ref. 5), especially at lower energies where the interaction with hydrogen predominates. The low predicted efficiencies for neutron energies of about 25 to 40 MeV probably reflect our inadequate knowledge of the neutron–carbon inelastic cross sections.

Finally, many of the above conclusions are strengthened by the results of our measurement of the n–p differential cross section[1]) which stimulated the present investigation. Using the predictions of Kurz for a 4.2 MeV threshold and for neutron energies below about 30 MeV gives cross sections which are in disagreement (≈ 10%) both with reasonable phase-shift results and with measurements in which no neutron detector was used. Substituting either the corresponding predictions of Stanton or the measured efficiencies yields reasonable results. Above 30 MeV the indications are less clear, with the n–p measurements weighing against both the predictions of Kurz and against the highest-energy data point, probably favoring results somewhere between Stanton's prediction and the measured results.

In summary, the ±5% (Stanton) and ±10% (Kurz) quoted by the authors[3, 5] as the accuracies of their predictions are in general reasonable, though at certain neutron energies the errors may be as much as twice these estimates. A better knowledge of the cross sections for the neutron–carbon inelastic reactions in the energy range 20 to 50 MeV would almost certainly improve the predictions.

Fig. 2. Measured efficiencies at 1.0 and 4.2 MeV thresholds, compared with the predictions of Stanton and Kurz.

References

1) T. C. Montgomery, F. P. Brady, B. E. Bonner, W. B. Broste and M. W. McNaughton, Phys. Rev. Letters **31** (1973) 640.
2) J. A. Jungerman and F. P. Brady, Nucl. Instr. and Meth. **89** (1970) 167.
3) R. J. Kurz, LRL report UCRL 11339 (1964).
4) S. T. Thornton and J. R. Smith, Nucl. Instr. and Meth. **96** (1971) 551.
5) N. R. Stanton, A Monte Carlo program for calculating neutron detection efficiencies in plastic scintillator, Ohio State University, preprint COO-1545-92 (1971).
6) C. E. Wiegand et al., Rev. Sci. Instr. **33** (1962) 526.
7) J. C. Young et al., Nucl. Instr. and Meth. **68** (1969) 333.
8) D. G. Crabb et al., Nucl. Instr. and Meth. **48** (1967) 87.
9) J. B. Hunt et al., Nucl. Instr. and Meth. **85** (1970) 269.
10) A. S. L. Parsons et al., Nucl. Instr. and Metn. **79** (1970) 43.